

# Generation of continuously tunable fractional optical orbital angular momentum using internal conical diffraction

D. P. O'Dwyer, C. F. Phelan, Y. P. Rakovich, P. R. Eastham, J. G. Lunney, and J. F. Donegan\*

*School of Physics, Trinity College Dublin, Dublin 2, Ireland*

*\* Principal Investigator, CRANN Research Institute, Trinity College Dublin, Ireland  
jdonegan@tcd.ie*

**Abstract:** When a left-circularly polarised Gaussian light beam, which has spin angular momentum (SAM)  $J_{\text{sp}} = \sigma\hbar = 1\hbar$  per photon, is incident along one of the optic axes of a slab of biaxial crystal it undergoes internal conical diffraction and propagates as a hollow cone of light in the crystal. The emergent beam is a superposition of equal amplitude zero and first order Bessel like beams. The zero order beam is left-circularly polarised with zero orbital angular momentum (OAM)  $J_{\text{orb}} = \ell\hbar = 0$ , while the first order beam is right-circularly polarized but carries OAM of  $J_{\text{orb}} = 1\hbar$  per photon. Thus, taken together the two beams have zero SAM and  $J_{\text{orb}} = \frac{1}{2}\hbar$  per photon. In this paper we examine internal conical diffraction of an elliptically polarised beam, which has fractional SAM, and demonstrate an all-optical process for the generation light beams with fractional OAM up to  $\pm 1\hbar$

©2010 Optical Society of America

**OCIS codes:**(350.5030) Phase; (260.1440) Birefringence; (260.1180) Crystal optics; (050.1940) Diffraction.

---

## References and links

1. L. Allen, S. M. Barnett, and M. J. Padgett, *Optical Angular Momentum* (Institute of Physics Publishing, 2003).
2. S. Franke-Arnold, L. Allen, and M. Padgett, "Advances in optical angular momentum," *Laser Photonics Rev.* **2**(4), 299–313 (2008).
3. D. McGloin, and K. Dholakia, "Bessel beams: diffraction in a new light," *Contemp. Phys.* **46**(1), 15–28 (2005).
4. J. Arlt, K. Dholakia, L. Allen, and M. J. Padgett, "The production of multiringed Laguerre–Gaussian modes by computer-generated holograms," *J. Mod. Opt.* **45**(6), 1231–1237 (1998).
5. C. Rotschild, S. Zommer, S. Moed, O. Hershcovitz, and S. G. Lipson, "Adjustable spiral phase plate," *Appl. Opt.* **43**(12), 2397–2399 (2004).
6. E. Karimi, B. Piccirillo, E. Nagali, L. Marrucci, and E. Santamato, "Efficient generation and sorting of orbital angular momentum eigenmodes of light by thermally tuned q-plates," *Appl. Phys. Lett.* **94**(23), 231124 (2009).
7. L. Marrucci, C. Manzo, and D. Paparo, "Optical spin-to-orbital angular momentum conversion in inhomogeneous anisotropic media," *Phys. Rev. Lett.* **96**(16), 163905 (2006).
8. T. A. King, W. Hogervorst, N. S. Kazak, N. A. Khilo, and A. A. Ryzhevich, "Formation of higher-order Bessel light beams in biaxial crystals," *Opt. Commun.* **187**(4-6), 407–414 (2001).
9. C. F. Phelan, D. P. O'Dwyer, Y. P. Rakovich, J. F. Donegan, and J. G. Lunney, "Conical diffraction and Bessel beam formation with a high optical quality biaxial crystal," *Opt. Express* **17**(15), 12891–12899 (2009).
10. J. Arlt, and K. Dholakia, "Generation of high-order Bessel beams by use of an axicon," *Opt. Commun.* **177**(1-6), 297–301 (2000).
11. J. Durmin, "Exact solutions for nondiffracting beams. I. The scalar theory," *J. Opt. Soc. Am. A* **4**(4), 651–654 (1987).
12. M. V. Berry, "Optical currents," *J. Opt. A, Pure Appl. Opt.* **11**(9), 094001 (2009).
13. J. B. Götte, K. O'Holleran, D. Preece, F. Flossmann, S. Franke-Arnold, S. M. Barnett, and M. J. Padgett, "Light beams with fractional orbital angular momentum and their vortex structure," *Opt. Express* **16**(2), 993–1006 (2008).
14. C. H. J. Schmitz, K. Uhrig, J. P. Spatz, and J. E. Curtis, "Tuning the orbital angular momentum in optical vortex beams," *Opt. Express* **14**(15), 6604–6612 (2006).

15. S. S. R. Oemrawsingh, X. Ma, D. Voigt, A. Aiello, E. R. Eliel, G. W. 't Hooft, and J. P. Woerdman, "Experimental demonstration of fractional orbital angular momentum entanglement of two photons," *Phys. Rev. Lett.* **95**(24), 240501 (2005).
16. A. Vaziri, G. Weihs, and A. Zeilinger, "Superpositions of the orbital angular momentum for applications in quantum experiments," *J. Opt. B Quantum Semiclassical Opt.* **4**(2), 367 (2002).
17. W. R. Hamilton, "Third supplement to an essay on the theory of systems of rays," *Transactions of the Royal Irish Academy*, 1–144 (1837).
18. H. Lloyd, "On the phenomena presented by light in its passage along the axes of biaxial crystals," *Phil. Mag* **1**, 112–120 and 207–210 (1833).
19. A. M. Belskii, and A. P. Khapalyuk, "Internal conical refraction of bounded light beams in biaxial crystals," *Opt. Spectrosc.* **44**, 312–315 (1978).
20. M. V. Berry, "Conical diffraction asymptotics: fine structure of Poggendorff rings and axial spike," *J. Opt. A, Pure Appl. Opt.* **6**(4), 289–300 (2004).
21. M. V. Berry, M. R. Jeffrey, and J. G. Lunney, "Conical diffraction: observations and theory," *Proc. R. Soc. Lond. A* **462**(2070), 1629–1642 (2006).
22. M. V. Berry, M. R. Jeffrey, and M. Mansuripur, "Orbital and spin angular momentum in conical diffraction," *J. Opt. A, Pure Appl. Opt.* **7**(11), 685–690 (2005).
23. D. Kasprowicz, M. Drozdowski, A. Majchrowski, and E. Michalski, "Spectroscopic properties of  $\text{KGd}(\text{WO}_4)_2$ : (Er, Yb) single crystals studied by Brillouin scattering method," *Opt. Mater.* **30**(1), 152–154 (2007).
24. M. J. Padgett, and J. Courtial, "Poincaré-sphere equivalent for light beams containing orbital angular momentum," *Opt. Lett.* **24**(7), 430–432 (1999).
25. W. C. Soares, D. P. Caetano, and J. M. Hickmann, "Hermite-Bessel beams and the geometrical representation of nondiffracting beams with orbital angular momentum," *Opt. Express* **14**(11), 4577–4582 (2006).

---

## 1. Introduction

In general, a light beam may have both spin angular momentum (SAM) and orbital angular momentum (OAM). The SAM per photon is  $J_{\text{sp}} = \sigma\hbar$  and is related to the state of polarization for left-circular  $\sigma = +1$ , for right-circular  $\sigma = -1$ , while for linearly polarised light  $\sigma = 0$ . For elliptically polarised light,  $J_{\text{sp}}$  varies from zero to  $\pm\hbar$  as the state of polarisation varies from linear to circular. Thus non-integer values of  $\sigma$  can readily be obtained. A Gaussian beam can only carry SAM.

Higher order beam modes such as Laguerre-Gaussian or high order Bessel beams can possess OAM due to the presence of an azimuthal phase factor  $e^{i\ell\theta}$ , where  $\theta$  is the azimuthal angle measured around the beam axis and  $\ell$  is the azimuthal mode index [1–3]. This factor corresponds to an optical vortex of topological charge  $\ell$ , in which the phase winds by  $2\pi\ell$  on a closed path around the beam. Experimentally, beams with OAM can be generated via numerous methods such as computer-generated fork holograms [4], spiral phase plates [5], q-plates [6,7], and internal conical diffraction [8,9]. Bessel beams are of special interest due to their properties of divergence-less propagation and self-repair [3]. They can be generated using internal conical diffraction [8,9], refraction by an axicon [10] or using an annular slit and positive lens combination [11].

For a scalar beam with an azimuthally symmetric intensity profile the OAM per photon is  $J_{\text{orb}} = \ell\hbar$ , where  $\ell$  is the total topological charge. Thus since the topological charge is necessarily an integer, the OAM of such a beam is quantized. However, in more general cases the OAM is not necessarily connected to the topological charge of the vortices [12], allowing for beams with fractional OAM. Such beams have been created by superposing Laguerre-Gaussian beams of different strength and vortex charge [13,14], as well as by using spiral wave plates [5] and q-plates [6]. In a quantum description such beams are superpositions of states of different OAM, so that the expectation value of OAM varies continuously.

In this paper, we describe how a relatively simple and robust all-optical setup, based on internal conical refraction, can be used to produce a light beam with continuously tunable OAM between 0 and  $\pm\hbar$  per photon. This all optical arrangement will provide a rapidly switchable method for the generation of high quality beams with fractional OAM, at the expense of high efficiency. These high quality beams may find use in optical trapping where the rotational frequency of a confined particle is known to be directly proportional to the

OAM [14]. Fractional beams provide a discrete multi-dimensional state space for photons, which may find applications in quantum information processing and encryption [15,16].

## 2. Conical diffraction of a Gaussian beam

When a monochromatic light beam is incident on a biaxial crystal, ( $n_1 < n_2 < n_3$ ), such that the wave vector lies along one of the two optic axes then the beam spreads out as a cone in the crystal and emerges as a double-ringed cylindrical beam. Conical refraction was predicted by Hamilton [17] in 1832 and experimentally observed by Lloyd shortly afterwards [18]. For a light beam of finite size it is necessary to account for the corresponding angular spread of the wave vector, therefore it is necessary to treat conical refraction as a diffraction problem. The wave theory of conical diffraction in the paraxial approximation was first treated by Belskii and Khapalyuk [19]. Berry extended this work by showing that the crystal may be represented as a linear operator that transforms the transverse field of the incident light beam [20,21].

A conically diffracted beam can be represented as the superposition of two beams that are associated with Bessel functions of zero ( $B_0$ ) and first order ( $B_1$ ), whose phase and electric field distribution is directly dependent on the input polarisation ( $e_x, e_y$ ), and is described by Eq. (1)a):

$$\mathbf{E}(\mathbf{R}, Z) = B_0(R, R_0, Z) \begin{pmatrix} e_x \\ e_y \end{pmatrix} + B_1(R, R_0, Z) \begin{pmatrix} \cos\theta & \sin\theta \\ \sin\theta & -\cos\theta \end{pmatrix} \begin{pmatrix} e_x \\ e_y \end{pmatrix}, \quad (1a)$$

$$B_0(R, R_0, Z) = k \int_0^\infty P \cos(kPR_0) a(P) J_0(kPR) e^{-\frac{1}{2}ikP^2Z} dP, \quad (1b)$$

$$B_1(R, R_0, Z) = k \int_0^\infty P \sin(kPR_0) a(P) J_1(kPR) e^{-\frac{1}{2}ikP^2Z} dP, \quad (1c)$$

where  $w$  is the beam waist,  $J_0(kPR)$  and  $J_1(kPR)$  are the Bessel functions of zero and first-order and  $a(P)$  is the Fourier transform of the transverse profile of the incident field.  $R_0 = AL$  is the radius of the conically diffracted beam in the focal image plane, where the crystal anisotropy factor  $A = \frac{1}{n_2} \sqrt{(n_3 - n_2)(n_2 - n_1)}$  and  $L$  is the length of the crystal. The individual beam profiles  $B_0(R, R_0, Z)$  and  $B_1(R, R_0, Z)$  satisfy the free space paraxial wave equation and have been shown to correspond very closely to experiment [9]. For a left-circularly polarised Gaussian beam input the  $B_0$  component is polarised in the same sense with  $J_{sp} = +1\hbar$  but zero OAM, while the  $B_1$  is right-circularly polarised ( $J_{sp} = -1\hbar$ ) and  $J_{orb} = +1\hbar$ . Thus taken together, the combined beam has zero SAM, but OAM of  $+ \frac{1}{2}\hbar$  per photon. This transformation of SAM to OAM in conical diffraction is discussed in more detail by Berry [22]. Since the  $B_0$  and  $B_1$  fields have opposite circular polarisation a circular analyser can be used to isolate  $B_1$ , which has OAM of  $1\hbar$  per photon and half the optical power of the incident beam.

This property of conical diffraction, which converts a Gaussian beam with SAM into a  $B_1$  beam with OAM of the same magnitude, also facilitates the generation of non-integer OAM in the range 0 to  $1\hbar$  per photon. This can be achieved using an elliptically polarised input beam, which corresponds to non-integer SAM. An elliptically-polarised beam is produced when a quarter-wave plate is placed in a linearly polarised beam so that the incident polarisation makes an angle  $\alpha$  with the fast axis. The SAM per photon,  $J_{sp}$ , is given by Eq. (2):

$$J_{sp} = \sigma\hbar = \hbar \frac{-i(E_x E_y^* - E_y E_x^*)}{|E_x|^2 + |E_y|^2} = \hbar \sin(2\alpha). \quad (2)$$

As  $\alpha$  is changed from  $0^\circ$  to  $45^\circ$  the polarisation of the input beam changes from linear with zero SAM, through elliptical with fractional SAM, to circular with SAM of  $1\hbar$ .

### 3. Experiment

A 10 mW 632 nm Gaussian laser beam linearly polarised in the horizontal plane was focused using a 5 cm lens to a beam waist size of 52  $\mu\text{m}$  near the input face of a 3 cm slab of the biaxial crystal  $\text{KGd}(\text{WO}_2)_4$ , supplied by CROptics©. At 632 nm the refractive indices are:  $n_1 = 2.01169$ ,  $n_2 = 2.042198$  and  $n_3 = 2.09510$  [23]. The crystal was then oriented so that the light is incident along one of the optic axes, which lies normal to the input face. Internal conical diffraction generates a double ring-shaped beam with radius  $R_0 = 5.9 \times 10^{-4}$  m and  $\rho_0 = R_0/w = AL/w = 11.3$ . The experimental set-up is shown in Fig. 1. A  $\lambda/2$  plate was used to rotate the plane of polarisation relative to the fast axis of the  $\lambda/4$  plate (P1) which was also oriented to be horizontal. The azimuthal orientation of the biaxial crystal was chosen so that the plane containing the two optic axes also lies in the horizontal plane.

To select the  $B_1$  beam a  $\lambda/4$  plate (P2) and linear polariser were placed after the crystal. The fast axis of wave plate P2 was set orthogonal to the fast axis of P1 and the output linear polariser (LP) was rotated so that it is always orthogonal to the linear polarisation incident on P1. If  $\alpha$  is the angle of the input linear polarisation relative to the fast axis of P1, then the polarisation of the light incident on the crystal changes from linear for  $\alpha = 0^\circ$ , through elliptical, to left-circular for  $\alpha = 45^\circ$ . Using matrix algebra to describe the operations of the various elements of the setup and Eq. (1a) for the operation of the crystal, it can be shown that for a given angle  $\alpha$ , the output optical field is given by:

$$\mathbf{E}(\mathbf{R}, Z) = B_1(R, R_0, Z) [\cos\theta \sin 2\alpha - i \sin\theta] \begin{pmatrix} \sin\alpha \\ -\cos\alpha \end{pmatrix}. \quad (3)$$

Thus, it can be seen that the output circular analyser only transmits the  $B_1$  component of the field generated by the crystal. In the case of  $\alpha = 45^\circ$  the polarisation into the crystal is left-circular. The square bracket in Eq. (3) reduces to  $e^{-i\theta}$ , which describes a  $2\pi$  azimuthal phase change. The last term indicates that the linear polarisation at the output is orthogonal to the input linear polarisation. Thus the output beam is linearly polarised but carries OAM of  $1\hbar$  per photon. For  $\alpha = 0^\circ$  the light into the crystal is polarised horizontally and the square bracket in Eq. (3) reduces to  $-i \sin\theta$ . As before, the output is linearly polarised, but now the OAM is zero and there is a  $\sin^2\theta$  azimuthal variation of intensity, with the zero intensity along the horizontal plane, which corresponds to  $\theta = 0^\circ$ .

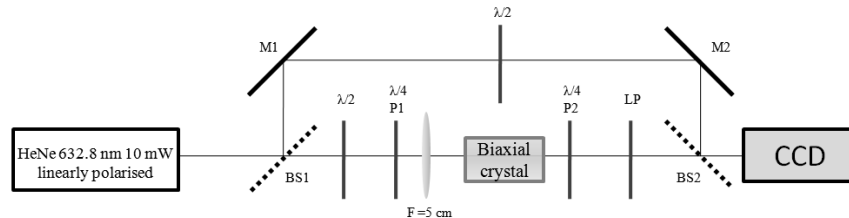


Fig. 1. Optical setup to generate a light beam with fractional OAM, and also including a Mach-Zehnder interferometer to record the phase distribution. (See text for explanation)

The optical setup also included a Mach-Zehnder interferometer to examine the phase distribution of the output beam as the polarisation into the crystal was changed. The beam in the reference arm is Gaussian and its polarisation was rotated through  $90^\circ$  so that it has the same polarization as the output beam. The intensity distributions and fringe patterns were recorded using a CCD camera. The camera is in the far-field region of the conically diffracted beam, i.e. the region where the ring-shaped beam has undergone diffraction to generate a superposition of conically diffracting beams described by Bessel functions [9,21].

### 4. Results and discussion

We first examined the phase distribution by setting the reference beam collinear with the output beam. Figure 2(i) shows the interference pattern for  $\alpha = 45^\circ$ , i.e. left-circular light into

the crystal. As expected the fringe pattern is a spiral, indicative of an optical field with  $J_{\text{orb}} = +1\hbar$  per photon. The output and reference beams were then slightly misaligned to generate a wedge fringe pattern. Figure 2(ii-iii) shows the wedge fringe patterns for  $\alpha = 0^\circ$  and  $45^\circ$  and Fig. 2(iv-v) shows a Mathematica simulation of the same interference patterns. As expected, the wedge fringe pattern Fig. 2(iii) for circular polarisation input  $\alpha = 45^\circ$  shows the expected single fringe dislocation indicative of a beam with  $\ell = 1$  [2].

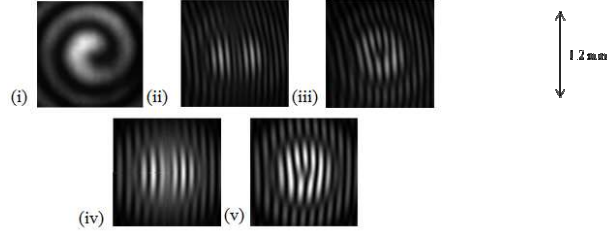


Fig. 2. (i) Collinear interference of Gaussian beam with output beam for circularly polarised input. Wedge fringe patterns for non-collinear interference of Gaussian beam with output beam for (ii)  $\alpha = 0^\circ$  and (iii)  $\alpha = 45^\circ$ . (iv-v) Mathematica simulation of (ii) and (iii).

The intensity distributions as the angle  $\alpha$  was changed from  $0^\circ$  to  $45^\circ$  were also measured. These are shown in Fig. 3(a), while Fig. 3(b) shows the same intensity distributions calculated using Mathematica using Eq. (3). Linear polarisation into the crystal  $\alpha = 0^\circ$  generates a 1st order Hermite-Bessel ( $\text{HB}_{01}$ ) beam Fig. 3(a-i), with zero intensity on the same axis as the direction of the incident polarisation; there is no fork dislocation in the wedge fringe pattern-Fig. 2(ii) indicates that there is no OAM present. As  $\alpha$  is increased from  $0^\circ$  to  $45^\circ$  the beam evolves from a Hermite-Bessel ( $\text{HB}_{01}$ ) distribution to the 1st order Bessel distribution Fig. 3(a-vi).

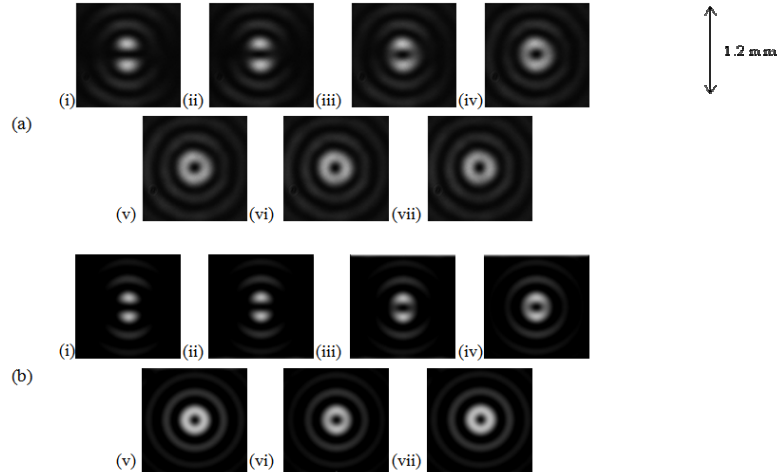


Fig. 3. Measured (a) and simulated (b) intensity distributions of the output beam as the polarisation of the input to the crystal is changed by setting the angle  $\alpha$  of the linear polarisation relative to the fast axis of the phase plate P1 to the following values:(i)  $0^\circ$ , (ii)  $8^\circ$ , (iii)  $16^\circ$ , (iv)  $24^\circ$ , (v)  $32^\circ$ , (vi)  $40^\circ$  and (vii)  $45^\circ$ .(b) Mathematica simulation of the intensity patterns in (a) using Eq. (3).

Following Berry [22], the angular momentum per photon of a light beam is given by

$$J = \frac{\hbar \text{Im} \iint dR (\mathbf{E}^* \cdot \partial_\theta \mathbf{E} + e_z \cdot \mathbf{E}^* \times \mathbf{E})}{\iint dR \mathbf{E}^* \cdot \mathbf{E}}, \quad (4)$$

where the first term gives the OAM and the second the SAM. Applying this equation to Eq. (3) yields the dependence of the OAM on wave-plate angle  $\alpha$  (incident SAM  $J_{sp}$ ):

$$J_{orb} = \hbar \frac{2\sin(2\alpha)}{\sin^2(2\alpha)+1} = J_{sp} \frac{2}{\sin^2(2\alpha)+1}. \quad (5)$$

Since the  $B_1$  field is linearly polarised, the SAM is zero. For  $\alpha = (0^\circ, 8^\circ, 16^\circ, 24^\circ, 32^\circ, 40^\circ, 45^\circ)$  the orbital angular momentum expectation value  $J_{orb} = (0, 0.276, 0.827, 0.852, 0.957, 0.994, 0.999, 1)$   $\hbar$  per photon. The relationship between input SAM and the output OAM can be understood by noting (from Eq. (3)) that the power in the transmitted beam varies as  $(\sin^2(2\alpha) + 1)/2$ . For  $\alpha = 45^\circ$  the optical power is split nearly equally between the  $B_0$  (blocked) and  $B_1$  (transmitted) fields. Thus at  $\alpha = 0^\circ$  the power in the transmitted field is one-quarter of the input power, whereas at  $\alpha = 45^\circ$  it is one-half.

The variation of the output beam OAM with input polarisation can also be understood in terms of the superposition of Hermite-Bessel beams [24–25]. For  $\alpha = 0^\circ$  the polarisation into the crystal is linear and the output is a Hermite-Bessel beam with zero OAM. However, for  $\alpha = 45^\circ$  the polarisation into the crystal is circular, which may be regarded as a superposition of two equal amplitude orthogonal linear states with a  $\pi/2$  phase difference. These two linear states generate orthogonal Hermite-Bessel beams which together form a conically diffracting first order Bessel beam with OAM.

## 6. Conclusion

We have shown how internal conical refraction of elliptically polarised light can be used to generate a beam with continuously variable fractional OAM in the range 0 to  $1\hbar$  per photon. The value of OAM is varied in a relatively simple way by congruent rotation of a  $\lambda/2$  plate, to tune the ellipticity of the input, with a biaxial crystal and a linear polariser at the output end. This technique may find application in the generation of beams with controllable OAM. Such control would be useful in optical trapping experiments and as an easily controllable source for optical computing.

## Acknowledgements

We acknowledge support from SFI under research grants 06/RFP/PHY029 and 08/IN.1/11862 and helpful discussions with Sir Michael Berry and Kishan Dholakia.